Paramagnetic ^{1}H NMR spectroscopy to investigate the catalytic mechanism of radical S-adenosylmethionine enzymes

Francesca Camponeschi[1,2,†], Riccardo Muzzioli[1,2,3,†], Simone Ciofi-Baffoni[1,2], Mario Piccioli[1,2], and Lucia Banci[1,2,*]

[1]Magnetic Resonance Center CERM, University of Florence, Via Luigi Sacconi 6, 50019, Sesto Fiorentino, Florence, Italy.

[2]Department of Chemistry, University of Florence, Via della Lastruccia 3, 50019 Sesto Fiorentino, Florence, Italy.

[3]Present address: Department of Cancer Systems Imaging, The University of Texas MD Anderson Cancer Center, 1881 East Road, 3SCR4.3600, Unit 1907, Houston, TX 77054.

[†]These authors contributed equally to this work.

[*]Corresponding author:

Prof. Lucia Banci

Magnetic Resonance Center CERM

University of Florence

Via Luigi Sacconi 6

50019, Sesto Fiorentino, Florence, Italy

Tel: +39 055 4574273

Fax: +39 055 4574923

E-mail: banci@cerm.unifi.it

Abstract

Iron-sulfur clusters in radical S-adenosylmethionine (SAM) enzymes catalyze an astonishing array of complex and chemically challenging reactions across all domains of life. Here we showed that ^{1}H NMR spectroscopy experiments tailored to reveal hyperfine-shifted signals of metal-ligands is a powerful tool to monitor the binding of SAM and of the octanoyl-peptide substrate to the two [4Fe-4S] clusters of human lipoyl synthase. The paramagnetically shifted signals of the iron-ligands were specifically assigned to each of the two bound [4Fe-4S] clusters, and then used to examine the interaction of SAM and substrate molecules with each of the two [4Fe-4S] clusters of human lipoyl synthase. ^{1}H NMR spectroscopy can therefore contribute to the description of the catalityc mechanism of radical SAM enzymes.

Keywords

Lipoyl synthase; iron-sulfur proteins; enzyme mechanism; electron transfer; metallo enzyme.

Lipoyl synthase (LIAS in humans) is a member of the radical S-(5'-Adenosyl)-L-Methionine (SAM) superfamily of enzymes and uses two [4Fe-4S] clusters to catalyze the final step of the biosynthesis of the lipoyl cofactor [1-7]. The mechanism of lipoyl synthase consists of a two-step reaction where a protein-bound octanoyl chain is converted into lipoic acid by a consecutive insertion of two sulfur atoms at C6 and C8 positions of the octanoyl chain [8, 9]. The two [4Fe-4S] clusters are both involved in the catalytic mechanism [9, 10]. One of them (**Fig. 1**), typical of all radical SAM enzymes (hereafter named FeS_{RS}), performs a reductive cleavage of a SAM molecule to obtain methionine and a 5'-deoxyadenosyl radical (5′-dA•) [1]. The 5′-dA• radical serves to generate a radical on the octanoyl chain. The other cluster (usually defined as auxiliary cluster and named FeS_{aux} hereafter, **Fig. 1**) provides the inorganic sulfides to the formed octanoyl chain radical [5, 9-11]. The FeS_{RS} cluster is bound to a CX_3CX_2C motif, i.e. three iron ions are covalently bound to three Cys residues of the motif (Cys 137, Cys 141 and Cys 144 in LIAS) and the fourth iron ion, termed as catalytic iron ion, is exposed for the binding of SAM (**Fig. 1**) [12, 13]. The FeS_{aux} cluster is bound through a conserved CX_4CX_5C motif (Cys 106, Cys 111 and Cys 117 in LIAS) and a serine (Ser 345 in LIAS) (**Fig. 1**) [12, 13]. The complete turnover of lipoyl synthase requires two equivalents of SAM (one per sulfur insertion) and two sulfur atoms from the auxiliary cluster. Therefore, lipoyl synthase typically catalyzes no more than one turnover in *in vitro* reactions as a consequence of the FeS_{aux} cluster disruption [1, 14]. Recently, it was shown that the Fe-S cluster carrier protein NfuA from *Escherichia coli* can regenerate the auxiliary cluster of *E. coli* lipoyl synthase (LipA) after each turnover. In such a way, although the consumption of the FeS_{aux} cluster after each turnover, LipA can act catalytically upon the continuos supply of [4Fe-4S] clusters by NfuA [15]. On the other hand, this mechanism of action, i.e. the FeS_{aux} cluster disruption, implies the release of free iron and inorganic sulfide ions and it would seem to present a problem for the cell considering the high iron and sulfide toxicity. Thus, it is reasonable that several important chemical aspects remain to be answered in order to have a complete description of the various steps of the enzymatic cycle [16]. The most enigmatic questions

concerns how the second sulfur atom is inserted in the substrate and the ultimate fate of the degraded auxiliary cluster.

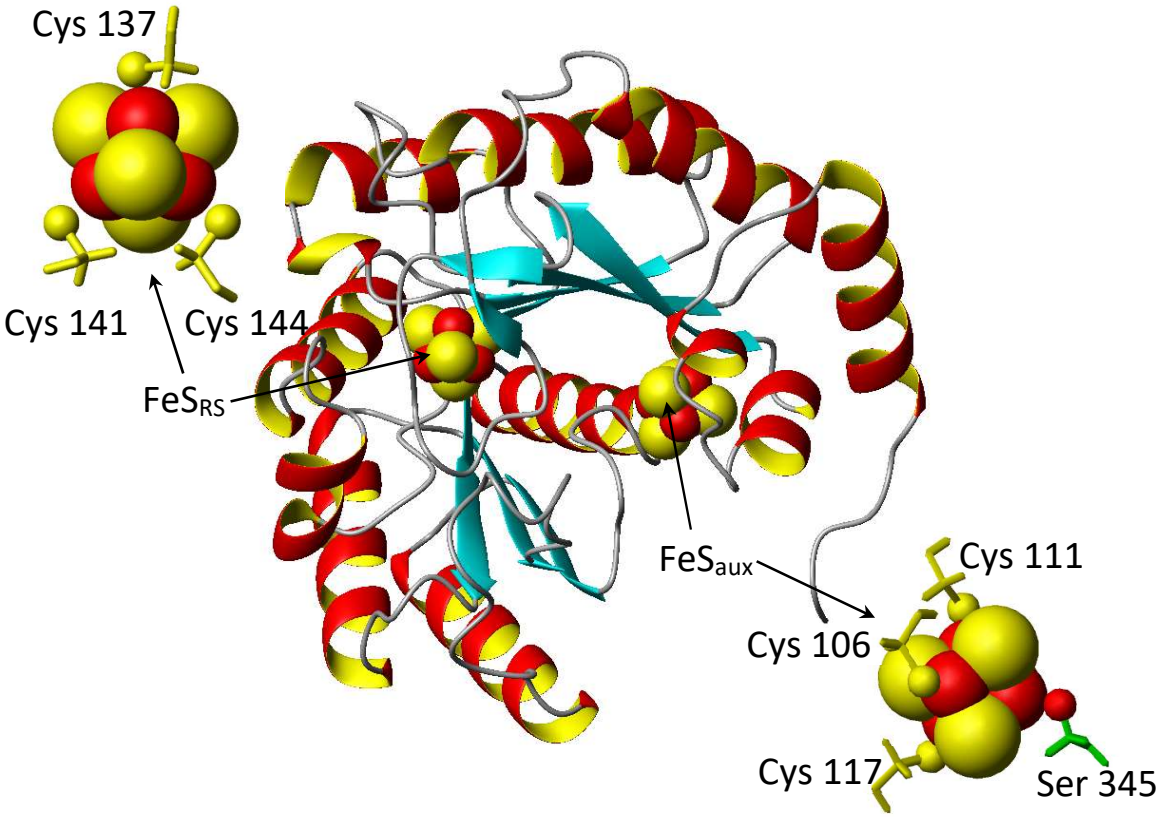

Figure 1. Structure of lipoyl synthase from *Mycobacterium tuberculosis* in ribbon representation (PDB ID 5EXJ). The FeS_{RS} and FeS_{aux} clusters and the iron ligands, numbered according to LIAS sequence, are shown in CPK mode and sticks, respectively.

This study reports for the first time that ^{1}H paramagnetic NMR spectroscopy is a valuable tool investigating the binding of SAM and substrate molecules to the two clusters of LIAS, in such a way resulting instrumental to contribute answering the still open questions of the enzymatic mechanism. To achieve this, we have exploited the hyperfine-shifted ^{1}H NMR signals of iron ligands of FeS_{RS} and FeS_{aux} clusters and follow their changes upon cluster interaction with SAM, with compounds mimicking SAM (S-(5'-Adenosyl)-L-Homocysteine, SAH) and the breakdown product of SAM (5'-deoxy-5'-MethylThioAdenosine, MTA), and with a synthetic

octanoyl-peptide substrate (Glu-Ser-Val-(N^6-octanoyl)Lys-Ala-Ala-Ser-Glu, named octanoyl-peptide hereafter) (**Fig. S1**).

Wild-type LIAS lacking the N-terminal mitochondrial targeting sequence was expressed and purified from *E. coli* cells (WT LIAS, hereafter). The protein was obtained highly pure and monomeric in solution (**Fig. 2a**) with a characteristic brown colour, displaying, in the UV-visible absorption spectrum, a weak shoulder at 330 nm and a broad peak at 400 nm, in addition to the peak at 280 nm due to aromatic amino acids (**Fig. 2b**). The peak at 400 nm is characteristic of $[4Fe\text{-}4S]^{2+}$ clusters with a delocalized redox state, i.e. with two $Fe^{2.5+}$-$Fe^{2.5+}$ pairs [17-19]. The UV-visible spectrum of WT LIAS does not significantly change upon its chemical reconstitution; consistently the signals in the paramagnetic ^1H NMR spectra of WT LIAS remain unperturbed before and after chemical reconstitution (data not shown). Therefore, the chemically reconstituted procedure was avoided for all WT LIAS samples used in the following spectroscopic characterization.

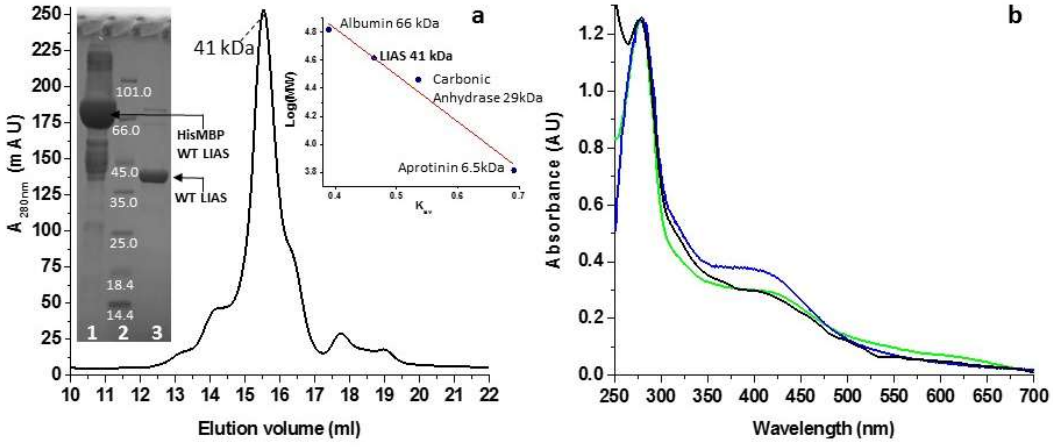

Figure 2. Analytical gel filtration and UV-visible absorption spectra of LIAS. (**a**) Analytical gel filtration chromatogram (protein concentration 500 μM) in 50 mM potassium phosphate, pH 7.0, with 5 mM DTT. The protein eluted at a volume corresponding to a molecular mass of 41 kDa. Right inset: Standard calibration curve for the Superdex 200 10/300 increase column. Left inset: SDS-PAGE of the last purification step of WT LIAS, 1. proteins obtained after the first HiTrap chelating column; 2. protein marker in kDa ; 3. protein obtained after TEV protease cleavage and a second passage on HiTrap chelating column. (**b**)

UV-visible absorption spectra of WT LIAS (blue line), chemically reconstituted C137/C141/C144A LIAS variant (green line), as purified C106/C111/C117A LIAS variant (black line). The buffer was 50 mM potassium phosphate, pH 7.0, with 5 mM DTT, and the sample concentration was 25 μM. The spectra were recorded in 1 cm cuvette.

The paramagnetic ^{1}H NMR spectrum of WT LIAS (**Fig. 3a**) shows two intense (***a*** and ***b***) and one weak (***c***) hyperfine shifted signals in the 20-13 ppm spectral region. Their size and linewidths are typical of βCH_2 and αCH of cysteine/serine bound to a $[4Fe\text{-}4S]^{2+}$ cluster [20-22]. The temperature dependence of hyperfine shifted NMR signals provides information on the electronic state of the paramagnetic center [23]. In the case of $[4Fe\text{-}4S]^{2+}$ clusters, the antiferromagnetic couplings among the four equivalent iron ions (each of them being formally $Fe^{2.5+}$) give rise to a S=0 diamagnetic ground state; the paramagentism arises from the excited levels of the energy diagram, that become more populated as temperature increases [24, 25]. The hyperfine shifts due to the contribution of the excited states therefore increase when increasing temperature, giving rise to the so-called antiCurie temperature dependence. Conversely, in the $[4Fe\text{-}4S]^{+}$ clusters which contain two $Fe^{2.5+}$ ions and two Fe^{3+} ions, magnetic couplings produce a paramagnetic S=1/2 ground state. Here, paramagentism decreases at increasing temperature and the chemical shifts follow the classical Curie law. As a consequence, the temperature dependence of ^{1}H NMR spectrum shown in **Fig. 3d** allowed us to obtain information about the oxidation state of the [4Fe-4S] clusters of LIAS. Signal ***a*** experiences an anti-Curie temperature dependence and the weak signal ***c*** exhibits a Curie temperature dependence (**Fig. 3d**). Temperature dependence of signal ***b*** suggests that at least two protons, having respectively Curie and anti-Curie temperature dependence, are overlapped in this signal (**Fig. 3d**). Longitudinal relaxation times (T_1) of signals ***a-d*** have been measured in WT LIAS in D_2O. T_1 values are in the 1-3 ms range (signal ***a***, 1.2 ± 0.2 ms; signal ***b***, 2.1 ms ± 0.4; signal ***c***, 2.5 ± 0.2 ms; signal ***d*** 1.6 ± 0.6 ms). They are slightly smaller than

previous findings in electron transfer Fe-S proteins [26-28] and account for electronic correlation time of iron ions around 1 x 10^{-11} s.

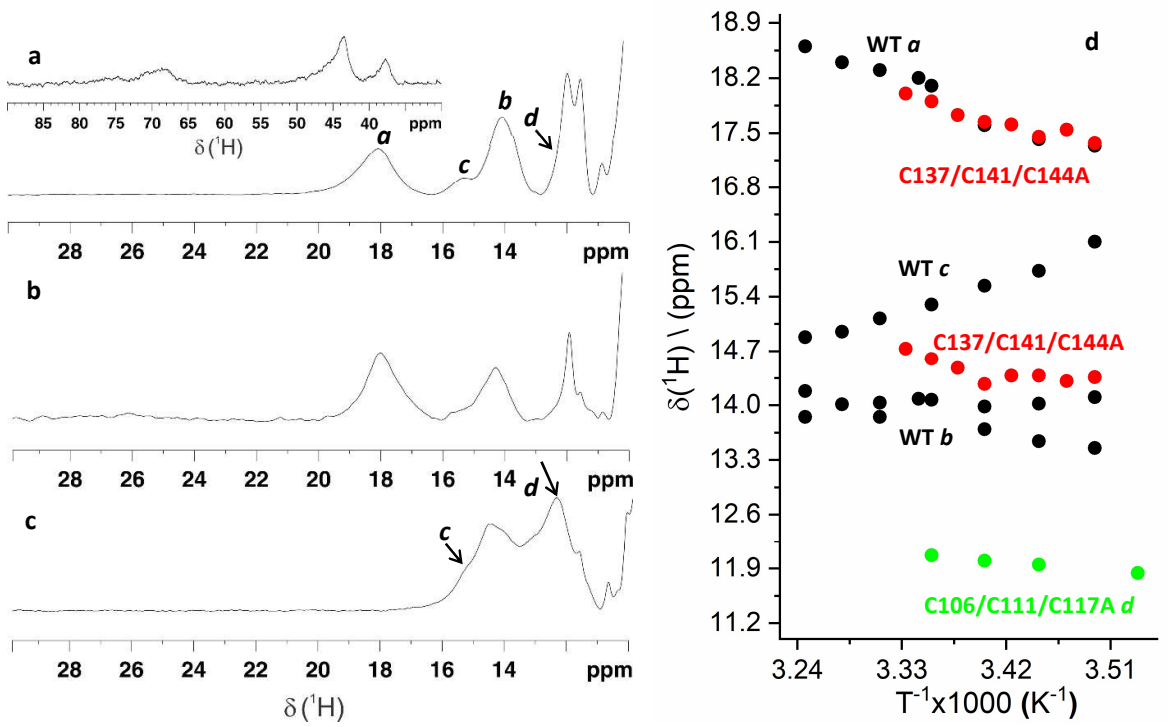

Figure 3. Paramagnetic ^{1}H NMR spectra of WT LIAS and of the triple LIAS variants and temperature dependence of hyperfine-shifted signals of cluster ligands. ^{1}H NMR spectra acquired at 400 MHz of: (**a**) WT LIAS in the 30-10 ppm spectral region and in the far-shifted 90-30 ppm region (*inset*), in degassed 50 mM phosphate buffer pH 7.0, and 5 mM DTT; (**b**) chemically reconstituted C137/C141/C144A LIAS variant in degassed 50 mM phosphate buffer pH 7.0, and 5 mM DTT; (**c**) as purified C106/C111/C117A LIAS variant in degassed 50 mM phosphate 100% D_2O buffer pH 7.0, and 5 mM DTT; (**d**) Temperature dependence of hyperfine-shifted signals of cysteine/serine ligands in WT LIAS (black dots) and triple C137/C141/C144A (red dots) and C106/C111/C117A (green dots) LIAS variants.

We used site-directed mutagenesis to obtain a cluster specific assignment of these NMR signals. In a LIAS variant, the three cysteine residues that binds the FeS_{RS} cluster (i.e. Cys 137, Cys 141 and Cys 144) were mutated into alanines; in another LIAS variant, the same type of mutations were performed on the FeS_{aux} cluster Cys ligands (i.e. Cys 106, Cys 111 and Cys 117). The triple C137/C141/C144A and C106/C111/C117A LIAS variants can thus

bind only the FeS_{aux} or the FeS_{RS} cluster, respectively. The UV-visible spectra of both variants are similar to that of WT LIAS, possessing the same distinctive features at 330 and 400 nm characteristic of $[4Fe\text{-}4S]^{2+}$ clusters and not displaying features that are indicative of $[2Fe\text{-}2S]^{2+}$ clusters (**Fig. 2b**). The paramagnetic ^1H NMR spectrum of the C137/C141/C144A LIAS variant shows two signals with chemical shift values very similar to those of the signals ***a*** and ***b*** observed in WT LIAS (**Fig. 3b**), both having an anti-Curie temperature dependence (**Fig. 3d**). The chemical shifts and the temperature dependence of these two signals are typical of βCH_2 of Cys or Ser residues bound to a $[4Fe\text{-}4S]^{2+}$ cluster with an S=0 electronic ground state. As previously reported for [4Fe-4S] and [2Fe-2S] clusters [22, 29], a Cys cluster ligand mutation to Ser affects the overall electronic distribution within the cluster but does not change dramatically the features of the ^1H NMR spectrum. Signals of serine βCH_2 will experience very similar hyperfine shift as cysteine βCH_2 signals. The shorter metal-to-proton distance of the oxygen-bound serine, compared to the sulfur-bound cysteine, may result in a faster nuclear relaxation of serine βCH_2; however, metal-to proton distances are affected also by Fe-S(O)-C-H dihedral angles and therefore we cannot discriminate between Cys and Ser ligands. However, comparing the paramagnetic ^1H NMR spectrum of the C137/C141/C144A LIAS variant, containing exclusively the auxiliary cluster, with those of wild-type $[4Fe\text{-}4S]^{2+}$ HIPIP and a stable variant $[4Fe\text{-}4S]^{2+}$ HiPIP in which a cysteine ligand had been replaced by serine ligand [22, 30, 31], it results that the chemical shift values observed for the beta protons of the auxiliary cluster are more similar to those reported for the mutated $[4Fe\text{-}4S]^{2+}$ HIPIP with respect to those of wild-type $[4Fe\text{-}4S]^{2+}$ HIPIP. This comparison suggest that Ser 345 is a ligand in the auxiliary cluster of human LIAS, in agreement with what observed in the crystal structures of bacterial LIAS homologues, in which the same serine was found to bind the auxiliary cluster [12, 13]. Moreover, signal ***a*** has a T_1 value smaller than what previously found for βCH_2 of cysteines bond to $[4Fe\text{-}4S]^{2+}$ cluster [26, 27], and this could be interpreted

as a further indirect evidence of serine coordination. In conclusion, all the NMR data on C137/C141/C144A LIAS variant allowed us to assign the ^{1}H signals due to the βCH_2 of Cys/Ser residues of the FeS_{aux} cluster in WT LIAS and to determine that the FeS_{aux} cluster is in an oxidized $[4Fe\text{-}4S]^{2+}$ state ($[4Fe\text{-}4S]_{aux}^{2+}$, hereafter). The paramagnetic ^{1}H NMR spectrum of the C106/C111/C117A LIAS variant contains two contiguous intense signals with very close chemical shifts that are similar to that of signal ***b*** observed in WT LIAS spectrum (**Fig. 3c**). As a result, the paramagnetic ^{1}H NMR spectra of both variants indicated that signal ***b*** in WT LIAS spectrum arises from three resonances and that one of these protons is due to FeS_{aux} cluster and the other two to the FeS_{RS} cluster. Both WT and C106/C111/C117A LIAS when dissolved in 100% D_2O buffer, which determines the disappearance of exchangeable signals, showed the presence of a signal (***d***) (**Fig. 3c**), which is hidden in the spectrum acquired in H_2O buffer by the sharp NH signal at 12.9 ppm (**Fig. 3a**). The anti-Curie temperature dependence of this signal (**Fig. 3d**) and its chemical shift are typical of a βCH_2 of a cysteine residue bound to an oxidized $[4Fe\text{-}4S]^{2+}$ cluster. A weak shoulder signal with the same chemical shift and Curie temperature dependence as those of the weak signal ***c*** observed in WT LIAS is also present in the paramagnetic ^{1}H NMR spectrum of the C106/C111/C117A LIAS variant (**Fig. 3c**). The detection of this Curie temperature dependent signal in the ^{1}H NMR spectra of both WT and C106/C111/C117A LIAS suggest that a small fraction of the FeS_{RS} cluster is in the reduced state. By comparing the chemical shift of this signal with known paramagnetic ^{1}H NMR spectra of small electron transfer reduced $[4Fe\text{-}4S]^{+}$ ferredoxins [32], it appears that signal ***c*** may arise from a αCH proton of a Cys residue bound to a reduced $[4Fe\text{-}4S]^{+}$ cluster. According to this interpretation, βCH_2 protons of cysteines bound to a $[4Fe\text{-}4S]^{+}$ cluster should be observed through a paramagnetic tailored experiment performed over a wide spectral window using fast repetition rates [33, 34]. Three very weak signals with Curie temperature dependence have been, indeed, detected, in the WT protein, in the 90-30 ppm

region (inset of **Fig. 3a**). Overall, the NMR data on the C106/C111/C117A LIAS variant allowed us to identify the ^{1}H signals due to the βCH_2 protons of the Cys residues of the FeS_{RS} cluster in WT LIAS, and indicated that the FeS_{RS} cluster in WT LIAS is mainly present in an oxidized $[4Fe\text{-}4S]^{2+}$ state ($[4Fe\text{-}4S]_{RS}^{2+}$ hereafter), and only a small fraction of the FeS_{RS} cluster is in a reduced $[4Fe\text{-}4S]^{+}$ state ($[4Fe\text{-}4S]_{RS}^{+}$ hereafter).

The NMR data described in the last paragraph on the variants were acquired i) on a C106/C111/C117A LIAS variant that was not chemically reconstituted since this variant is characterized by a low protein stability and largely precipitates upon chemical reconstitution, and ii) on a C137/C141/C144A LIAS variant that was, on the contrary, chemically reconstituted to form a $[4Fe\text{-}4S]^{2+}$ cluster, since the paramagnetic ^{1}H NMR spectrum of the as purified C137/C141/C144A LIAS variant shows signals of $\beta CH_2/\alpha CH$ cysteine ligands typical of a mixture of $[4Fe\text{-}4S]^{2+}$ a $[3Fe\text{-}4S]^{+}$ clusters [35, 36] with a 30/70 intensity ratio for the two species (**Fig. S2**). Overall, the NMR spectra on the two variants showed that a structural cooperativity is present between the two clusters. Indeed, the absence of the FeS_{RS} cluster exposes the FeS_{aux} cluster to oxidative conversion from $[4Fe\text{-}4S]^{2+}$ to $[3Fe\text{-}4S]^{+}$, and when FeS_{RS} cluster is the only cluster present in the enzyme, the protein stability is greatly reduced.

The cluster-specific assignment of the paramagnetic ^{1}H NMR signals of WT LIAS allowed us to follow the interactions of SAM and substrate molecules with the two [4Fe-4S] clusters of WT LIAS. We have first investigated the interaction of WT LIAS with SAM (**Fig. S1**). Stepwise additions of SAM to WT LIAS (up to two equivalents) give rise to a new set of intense peaks in the 22-13 ppm region (labelled with symbols ***α-δ*** in **Fig. 4a**), at decrement of signals ***b*** and ***c***, which contain resonances from the FeS_{RS} cluster ligands, while signal ***a*** of the FeS_{aux} cluster remains essentially unaffected by the SAM-LIAS interaction.

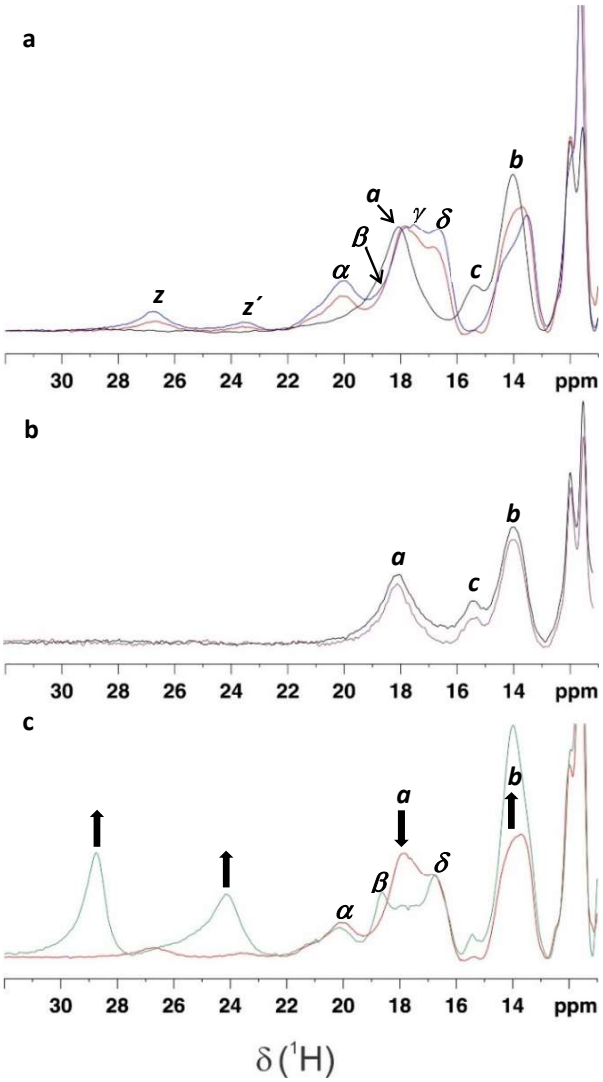

Figure 4. Paramagnetic ^{1}H NMR spectra of WT LIAS in the presence of SAM and the octanoyl-peptide substrate. ^{1}H NMR spectra acquired at 400 MHz of: (**a**) WT LIAS in the

absence (black) and in the presence of one (red) and two (blue) equivalents of SAM; (**b**) WT LIAS in the absence (black) and in the presence of one equivalent of octanoyl-peptide substrate (violet); (**c**) WT LIAS in the presence of one equivalents of SAM (red), and one equivalent of SAM and one equivalent of octanoyl-peptide substrate (green). Sample conditions are degassed 50 mM phosphate buffer pH 7.0, and 5 mM DTT.

All the new α-δ signals have chemical shift values and anti-Curie temperature dependences consistent with a new species containing a $[4Fe\text{-}4S]^{2+}$ cluster (**Fig. S3**). All these data indicated the formation of a SAM-LIAS adduct in which SAM closely interacts with the $[4Fe\text{-}4S]_{RS}^{2+}$ cluster, while it is not interacting with FeS_{aux} cluster. This is in agreement with previous ENDOR studies showing that SAM binds to radical SAM Fe-S cluster via coordination of the amino and carboxylate of SAM to the catalytic iron ion of the $[4Fe\text{-}4S]_{RS}^{2+}$ cluster [37, 38], and with the crystal structure of LipA complexed with the SAM-mimic compound SAH (**Fig. S1**), which showed that SAH is located close to the FeS_{RS} cluster while being far from the FeS_{aux} cluster [13]. Consistent with this analysis, the same spectral changes were observed when monitoring the interaction between WT LIAS and the SAM-mimic compound SAH, i.e. signals with chemical shifts similar to those of the α-δ signals, all having anti-Curie temperature dependence, were observed (data not shown). Moreover, the stepwise disappearance of signal ***c*** in **Fig. 4a** indicate that the small fraction of reduced $[4Fe\text{-}4S]_{RS}^{+}$ cluster gets oxidized upon addition of SAM, as expected by the $[4Fe\text{-}4S]_{RS}^{+}$-induced reductive cleavage of SAM. No signals of βCH_2 of cysteines bound to the small fraction of reduced $[4Fe\text{-}4S]_{RS}^{+}$ cluster were indeed observed in the 70-30 ppm region in the final mixture, in agreement with the FeS_{RS} cluster oxidation.

In the interaction between WT LIAS and SAM, two signals **z** and **z'** at 26.9 and 23.5 ppm, having lower intensity than α-δ signals, appear by SAM additions. The chemical shift values and the anti-Curie temperature dependence of these two signals (**Fig. S3**) are consistent with

the formation of a $[4Fe\text{-}4S]^{2+}$ cluster species. The observed oxidation of the small fraction of $[4Fe\text{-}4S]_{RS}^{+}$ cluster induced by SAM addition produces the formation of methionine and of the 5′-dA• radical. This radical is a transient and higly reactive intermediate and was only very recently observed at low temperature using a novel approach involving cryogenic photoinduced electron transfer [38-40]. It is thus impossible that it would survive in these experiments long enough to produce interactions observable by NMR. Therefore, 5'-dAdo• is reasonably quenched upon production to generate 5'-deoxyadenosine (5′-dA). Bearing in mind that 5′-dA is expected to go close the FeS_{aux} cluster in order to form the radical on the octanoyl chain of the substrate, we can suggest that the ***z*** and ***z'*** signals originate from the βCH_2 of the cysteines bound to the 5′-dA-interacting FeS_{aux} cluster species. According to this interpretation, the low intensity of the ***z*** and ***z'*** signals with respect to the ***α-δ*** signals is in agreement with the low percentage of the reduced $[4Fe\text{-}4S]_{RS}^{+}$ cluster present in the protein that can promote SAM cleavage and thus form the 5′-dA-interacting species. To validate this model, the interaction between WT LIAS and a compound mimicking the 5′-dA (MTA, **Fig. S1**) was investigated. Unlike what we observed following the additions of SAM, an excess of MTA (up to 2.5 equivalents) was required to observe some spectral changes in WT LIAS. The formation of new signals with chemical shifts similar to those of ***α-δ*** signals was, however, not observed upon MTA additions (**Fig. S4**), thus indicating that MTA does not interact with FeS_{RS} cluster. However, two new weak signals at 26.8 and 23.7 ppm, with very similar chemical shift to the ***z*** and ***z'*** signals observed in the SAM-WT LIAS complex, appeared (**Fig. S4**). These new signals have chemical shift values and anti-Curie temperature dependences consistent with a $[4Fe\text{-}4S]^{2+}$ state, as the two signals ***z*** and ***z'*** have (**Fig. S3**). Considering that MTA is proximal to one iron ion of the FeS_{aux} cluster in the LipA crystal structure complexed with MTA [13], we conclude that these two signals originate from the presence of a species formed by the $[4Fe\text{-}4S]_{aux}^{2+}$ cluster interacting with MTA in the 1:2.5 WT LIAS-MTA mixture. This observation confirms the interpretation described above, i.e. 5′-dA and

methionine are formed by SAM cleavage by the small fraction of reduced FeS_{RS} cluster present in WT LIAS and the formed 5′-dA interacts with the FeS_{aux} cluster.

The interaction between WT LIAS and the octanoyl-peptide substrate mimicking the amino acid sequence of the glycine cleavage system H protein was followed by acquiring paramagnetic ^{1}H NMR spectra on a 1:1 mixture of WT LIAS and octanoyl-peptide, and on a 1:1:1 mixture of WT LIAS, octanoyl-peptide and SAM (sequential or simultaneous addition of SAM and octanoyl-peptide produce the same final ^{1}H NMR spectrum). The paramagnetic ^{1}H NMR spectrum of the 1:1 mixture of WT LIAS and octanoyl-peptide is fully superimposable with that of WT LIAS, indicating that the octanoyl-peptide does not interact with the protein in the absence of SAM (**Fig. 4b**). On the contrary, the paramagnetic ^{1}H NMR spectrum of the 1:1:1 mixture of WT LIAS, octanoyl-peptide and SAM shows several spectral changes. Specifically, two new intense signals at 28.8 and 24.1 ppm appear, signal ***b*** increases while signal ***a*** decreases in intensity (**Fig. 4c**). The two new signals have chemical shift values and anti-Curie temperature dependences consistent with the presence of $[4Fe\text{-}4S]^{2+}$ clusters in the mixture (**Fig. S3**). These spectral changes occur on signals of the FeS_{aux} cluster cysteines. Indeed, signal ***a*** is exclusively due to βCH_2 of cysteine/serine of the FeS_{aux} cluster, signal ***b*** includes βCH_2 of a cysteine/serine of the FeS_{aux} cluster, and the signals at 28.8 ppm and 24.1 ppm have chemical shift values similar to those of ***z*** and ***z'*** signals, which characterize the FeS_{aux} cluster interactions, as discussed above. Therefore, the observed spectral changes monitor the interaction between the octanoyl-peptide and the FeS_{aux} cluster. On the contrary, the signals ***α-δ*** assigned to the SAM-bound FeS_{RS} cluster remains essentially unperturbed (**Fig. 4c**), indicating that SAM remains bound to the cluster. Overall, the SAM:peptide:WT LIAS interaction studies indicate that, only once SAM is bound to the protein, the octanoyl-peptide substrate can recognize its binding site. This is in agreement with what found in the radical SAM enzyme biotin synthase, where dethiobiotin substrate binding occurs only in the presence of SAM and the substrate binding is highly cooperative [41].

In conclusion, the data here presented showed that ^{1}H NMR spectroscopy tailored to reveal hyperfine-shifted signals of metal-ligands [42] is a powerful tool to investigate the sequential binding of SAM and of the octanoyl-peptide substrate to the [4Fe-4S] clusters of human lipoyl synthase. We can specifically monitor the interaction between SAM and the FeS_{RS} cluster, the redox changes of the FeS_{RS} cluster upon SAM interaction, follow the reductive cleavage of SAM, and monitor the substrate binding at the FeS_{aux} cluster. These information can be exploited to characterize the catalytic mechanism of the radical SAM superfamily of enzymes. In particular, we believe that, while X-ray, EPR and ENDOR spectroscopies offer a more detailed but also more static view by trapping the intermediates of the catalytic mechanism and freezing transient interactions, paramagnetic NMR provides a picture at room temperature of the kinetics of substrate uptake and its transformation, as well as the dynamics of site specific interactions of SAM and the substrate occuring at both clusters, thus being essential to obtain a comprehensive view of the catalytic mechanism.

Acknowledgement

The authors acknowledge the support and the use of resources of Instruct-ERIC, a Landmark ESFRI project, and specifically CERM/CIRMMP Italy Centre. This article is based upon work from COST Action CA15133, supported by COST (European Co-operation in Science and Technology). Financial support of the Fondazione Cassa di Risparmio di Firenze (CRF20160985) is gratefully acknowledged.

Competing Interests.

The authors declare no competing financial interests.

Author Contributions

Conceptualization: L.B. and S.C.B.; Methodology: M.P.; Validation: F.C.; Investigation: M.P., R.M., F.C. and S.C.B.; Writing – Original Draft: S.C.B. and M.P. Writing – Review & Editing: M.P., R.M., F.C., S.C.B and L.B.; Visualization: R.M. and F.C. Supervision: M.P., S.C.B and L.B.; Funding Acquisition: M.P. and L.B.

Appendix A. Supplementary data

Supplementary information includes Materials and Methods and Supplementary Figures S1-S4.

References

[1] R.M. Cicchillo, D.F. Iwig, A.D. Jones, N.M. Nesbitt, C. Baleanu-Gogonea, M.G. Souder, et al. Lipoyl synthase requires two equivalents of S-adenosyl-L-methionine to synthesize one equivalent of lipoic acid. Biochemistry. 2004;43:6378-86.

[2] S.J. Booker, R.M. Cicchillo, T.L. Grove. Self-sacrifice in radical S-adenosylmethionine proteins. Curr Opin Chem Biol. 2007;11:543-52.

[3] E. Mulliez, V. Duarte, S. Arragain, M. Fontecave, M. Atta. On the Role of Additional [4Fe-4S] Clusters with a Free Coordination Site in Radical-SAM Enzymes. Frontiers in chemistry. 2017;5:17.

[4] M. Fontecave, S. Ollagnier-de-Choudens, E. Mulliez. Biological radical sulfur insertion reactions. Chem Rev. 2003;103:2149-66.

[5] J.R. Miller, R.W. Busby, S.W. Jordan, J. Cheek, T.F. Henshaw, G.W. Ashley, et al. Escherichia coli LipA is a lipoyl synthase: in vitro biosynthesis of lipoylated pyruvate dehydrogenase complex from octanoyl-acyl carrier protein. Biochemistry. 2000;39:15166-78.

[6] J.B. Broderick, B.R. Duffus, K.S. Duschene, E.M. Shepard. Radical S-adenosylmethionine enzymes. Chem Rev. 2014;114:4229-317.

[7] D.P. Dowling, J.L. Vey, A.K. Croft, C.L. Drennan. Structural diversity in the AdoMet radical enzyme superfamily. Biochim Biophys Acta. 2012;1824:1178-95.

[8] R.M. Cicchillo, K.H. Lee, C. Baleanu-Gogonea, N.M. Nesbitt, C. Krebs, S.J. Booker. Escherichia coli lipoyl synthase binds two distinct [4Fe-4S] clusters per polypeptide. Biochemistry. 2004;43:11770-81.

[9] P. Douglas, M. Kriek, P. Bryant, P.L. Roach. Lipoyl synthase inserts sulfur atoms into an octanoyl substrate in a stepwise manner. Angew Chem Int Ed Engl. 2006;45:5197-9.

[10] R.M. Cicchillo, S.J. Booker. Mechanistic investigations of lipoic acid biosynthesis in Escherichia coli: both sulfur atoms in lipoic acid are contributed by the same lipoyl synthase polypeptide. J Am Chem Soc. 2005;127:2860-1.

[11] F. Forouhar, S. Arragain, M. Atta, S. Gambarelli, J.M. Mouesca, M. Hussain, et al. Two Fe-S clusters catalyze sulfur insertion by radical-SAM methylthiotransferases. Nat Chem Biol. 2013;9:333-8.

[12] M.I. McLaughlin, N.D. Lanz, P.J. Goldman, K.H. Lee, S.J. Booker, C.L. Drennan. Crystallographic snapshots of sulfur insertion by lipoyl synthase. Proc Natl Acad Sci U S A. 2016;113:9446-50.

[13] J.E. Harmer, M.J. Hiscox, P.C. Dinis, S.J. Fox, A. Iliopoulos, J.E. Hussey, et al. Structures of lipoyl synthase reveal a compact active site for controlling sequential sulfur insertion reactions. Biochem J. 2014;464:123-33.

[14] N.D. Lanz, M.E. Pandelia, E.S. Kakar, K.H. Lee, C. Krebs, S.J. Booker. Evidence for a catalytically and kinetically competent enzyme-substrate cross-linked intermediate in catalysis by lipoyl synthase. Biochemistry. 2014;53:4557-72.

[15] E.L. McCarthy, S.J. Booker. Destruction and reformation of an iron-sulfur cluster during catalysis by lipoyl synthase. Science. 2017;358:373-7.

[16] E.L. McCarthy, S.J. Booker. Biochemical Approaches for Understanding Iron-Sulfur Cluster Regeneration in Escherichia coli Lipoyl Synthase During Catalysis. Methods Enzymol. 2018;606:217-39.

[17] J.C. Crack, J. Munnoch, E.L. Dodd, F. Knowles, M.M. Al Bassam, S. Kamali, et al. NsrR from Streptomyces coelicolor is a nitric oxide-sensing [4Fe-4S] cluster protein with a specialized regulatory function. J Biol Chem. 2015;290:12689-704.

[18] H. Beinert, R.H. Holm, E. Munck. Iron-sulfur clusters: nature's modular, multipurpose structures. Science. 1997;277:653-9.

[19] S.A. Freibert, B.D. Weiler, E. Bill, A.J. Pierik, U. Muhlenhoff, R. Lill. Biochemical Reconstitution and Spectroscopic Analysis of Iron-Sulfur Proteins. Methods Enzymol. 2018;599:197-226.

[20] L. Banci, F. Camponeschi, S. Ciofi-Baffoni, M. Piccioli. The NMR contribution to protein-protein networking in Fe-S protein maturation. Journal of Biological Inorganic Chemistry. 2018;23:665-85.

[21] I. Bertini, M.M.J. Couture, A. Donaire, L.D. Eltis, I.C. Felli, C. Luchinat, et al. The solution structure refinement of the paramagnetic reduced HiPIP I from *Ectothiorhodospira halophila* by using stable isotope labeling and nuclear relaxation. Eur J Biochem. 1996;241:440-52.

[22] E. Babini, I. Bertini, M. Borsari, F. Capozzi, A. Dikiy, L.D. Eltis, et al. A Serine -> Cysteine Ligand Mutation in the High Potential Iron-Sulfur Protein from *Chromatium vinosum* Provides Insight into the Electronic Structure of the [4Fe-4S] Cluster. J Am Chem Soc. 1996;118:75-80.

[23] I. Bertini, C. Luchinat, L. Messori. Nuclear relaxation in NMR of paramagnetic systems. In: Sigel H, editor. Metal ions in biological systems, vol 21 Applications of nuclear magnetic resonance to paramagnetic species. New York: Marcel Dekker, Inc.; 1987. p. 47-86.

[24] I. Bertini, F. Capozzi, S. Ciurli, C. Luchinat, L. Messori, M. Piccioli. Identification of the iron ions of HiPIP from *Chromatium vinosum* within the protein frame through 2D NMR experiments. J Am Chem Soc. 1992;114:3332-40.

[25] L. Banci, I. Bertini, C. Luchinat. The ^{1}H NMR parameters of magnetically coupled dimers - The Fe_2S_2 proteins as an example. Struct Bonding. 1990;72:113-35.

[26] I. Bertini, A. Gaudemer, C. Luchinat, M. Piccioli. Electron self-exchange in HiPIPs. A characterization of HiPIP I from *Ectothiorhodospira vacuolata*. Biochemistry. 1993;32:12887-93.

[27] I. Bertini, F. Briganti, C. Luchinat, A. Scozzafava, M. Sola. ^{1}H NMR spectroscopy and the electronic structure of the high potential iron-sulfur protein from *Chromatium vinosum*. J Am Chem Soc. 1991;113:1237-45.

[28] I. Bertini, F. Capozzi, C. Luchinat, M. Piccioli. ^{1}H NMR investigation of oxidized and reduced HiPIP from *R. globiformis*. Eur J Biochem. 1993;212:69-78.

[29] H. Cheng, B. Xia, G.H. Reed, J.L. Markley. Optical, EPR, and 1H NMR spectroscopy of serine-ligated [2Fe-2S] ferredoxins produced by site-directed mutagenesis of cysteine residues in recombinant Anabaena 7120 vegetative ferredoxin. Biochemistry. 1994;33:3155-64.

[30] S.S. Mansy, Y. Xiong, C. Hemann, R. Hille, M. Sundaralingam, J.A. Cowan. Crystal structure and stability studies of C77S HiPIP: a serine ligated [4Fe-4S] cluster. Biochemistry. 2002;41:1195-201.

[31] D. Bentrop, I. Bertini, F. Capozzi, A. Dikiy, L.D. Eltis, C. Luchinat. Three dimensional structure of the reduced C77S mutant of the *Chromatium vinosum* high potential iron-sulfur protein through NMR. Comparison with the solution structure of the wild-type protein. Biochemistry. 1996;35:5928-36.

[32] I. Bertini, F. Capozzi, C. Luchinat, M. Piccioli, A.J. Vila. The Fe_4S_4 centers in ferredoxins studied through proton and carbon hyperfine coupling. Sequence specific assignments of cysteines in ferredoxins from *Clostridium acidi urici* and *Clostridium pasteurianum*. J Am Chem Soc. 1994;116:651-60.

[33] J. Gaillard, J.-M. Moulis, J. Meyer. Hydrogen-1 nuclear magnetic resonance of selenium-substituted clostridial ferredoxins. Inorg Chem. 1987;26:320-4.

[34] A.L. Macedo, I. Moura, J.J.G. Moura, J. LeGall, B.H. Huynh. Temperature-dependent proton NMR investigation of the electronic structure of the trinuclear iron cluster of the oxidized *Desulfovibrio gigas* ferredoxin II. Inorg Chem. 1993;32:1101-5.

[35] S.C. Busse, G.N. La Mar, L.P. Yu, J.B. Howard, E.T. Smith, Z.H. Zhou, et al. Proton NMR Investigation of the Oxidized Three-Iron Clusters in the Ferredoxins from the Hyperthermophilic Archae *Pyrococcus furiosus* and *Thermococcus litoralis*. Biochemistry. 1992;31:11952-62.

[36] D. Bentrop, I. Bertini, C. Luchinat, J. Mendes, M. Piccioli, M. Teixeira. Paramagnetic NMR of the 7Fe ferredoxin from the hyperthermoacidophilic archaeon *Desulfurolobus ambivalens* reveals structural similarity to other dicluster ferredoxins. Eur J Biochem. 1996;236:92-9.

[37] C.J. Walsby, D. Ortillo, W.E. Broderick, J.B. Broderick, B.M. Hoffman. An anchoring role for FeS clusters: chelation of the amino acid moiety of S-adenosylmethionine to the unique iron site of the [4Fe-4S] cluster of pyruvate formate-lyase activating enzyme. J Am Chem Soc. 2002;124:11270-1.

[38] M. Horitani, K. Shisler, W.E. Broderick, R.U. Hutcheson, K.S. Duschene, A.R. Marts, et al. Radical SAM catalysis via an organometallic intermediate with an Fe-[5'-C]-deoxyadenosyl bond. Science. 2016;352:822-5.

[39] M. Horitani, A.S. Byer, K.A. Shisler, T. Chandra, J.B. Broderick, B.M. Hoffman. Why Nature Uses Radical SAM Enzymes so Widely: Electron Nuclear Double Resonance Studies of Lysine 2,3-Aminomutase Show the 5'-dAdo* "Free Radical" Is Never Free. J Am Chem Soc. 2015;137:7111-21.

[40] H. Yang, E. McDaniel, S. Impano, A.S. Byer, R.J. Jodts, K. Yokoyama, et al. The Elusive 5'-Deoxyadenosyl Radical: Captured and Characterized by EPR and ENDOR Spectroscopies. J Am Chem Soc. 2019.

[41] N.B. Ugulava, K.K. Frederick, J.T. Jarrett. Control of adenosylmethionine-dependent radical generation in biotin synthase: a kinetic and thermodynamic analysis of substrate binding to active and inactive forms of BioB. Biochemistry. 2003;42:2708-19.

[42] D. Brancaccio, A. Gallo, M. Piccioli, E. Novellino, S. Ciofi-Baffoni, L. Banci. [4Fe-4S] Cluster Assembly in Mitochondria and Its Impairment by Copper. J Am Chem Soc. 2017;139:719-30.